Molecular Orbital Model Studies of the Effect of Strain on Hyperconjugation in Carbonium Ions[1]

Andrew Streitwieser, Jr.,* and Spiro Alexandratos

Contribution from the Department of Chemistry, University of California, Berkeley, California 94720. Received March 7, 1977

Abstract: A systematic study aimed at clarifying the effect of strained C–C and C–H bonds on hyperconjugative stabilization of carbonium ions is presented. Ab initio theory at the STO-3G level was employed as was the semiempirical extended Hückel theory. Examination of the vinyl cation shows that decreasing the HCH bond angle of the methylene group leads to greater interaction with the empty p orbital. This interaction to give the corresponding bonding molecular orbital (BMO) and antibonding MO (ABMO) of the vinyl system is examined in detail at both levels of theory. The concept of hyperconjugative interaction is then put into the broader context of chemical reactivity by examining the formation of various carbonium ions in model reactions. The results show no simple relationship between overall energy changes in the model reactions and the changes in hyperconjugation interactions alone. These results also emphasize the limitations of theoretical conclusions based solely on HOMO and LUMO changes.

The relative stability of carbonium ions adjacent to strained carbon atoms has been interpreted in terms of enhanced hyperconjugative interaction.[2,3] Examples of such systems include the cyclopropylcarbinyl cation[4,5] and bicyclic cations such as the norbornyl cation.[6-8] Indeed, the controversial norbornyl cation system may simply involve an anisotropic bridgehead carbon which confers greater hyperconjugative stabilization to an essentially classical exo-2 cationic transition state than to a corresponding endo-2 transition state. In molecular orbital terms, enhanced hyperconjugative stabilization is equivalent to the orbital interactions expressed in Figure 1. Interaction of a higher energy (strained) σ orbital with the empty p orbital of a carbonium ion provides greater energy lowering than that of a lower energy σ orbital, assuming that the corresponding overlap integrals are comparable. This effect is a result of the well-known principle that the interaction of two wave functions is directly dependent on their overlap and inversely proportional to their energy difference.

This concept of enhanced hyperconjugative interaction as a function of strain is not only of substantial importance in its own right, but this type of orbital approach has become common in the modern electronic theory of organic chemistry. Accordingly, we present here a more thorough analysis of the interactions implied in Figure 1 with reference to SCF–MO calculations of several explicit systems.

Qualitatively, Figure 1 tells us that the antibonding molecular orbital (ABMO) of the more strained system should be of higher energy than the ABMO of the less strained system because of the greater interaction of the more strained σ bond with the p orbital; also, in spite of the enhanced splitting, the energy of the bonding molecular orbital (BMO) of the strained system probably remains higher than that of the BMO of the less strained system. One of the simplest systems with which

to investigate these considerations is the vinyl cation,[9] wherein we will be looking at the energy of interaction between the methylene moiety and the empty p orbital as function of angle strain at the CH_2 group. We will thus be looking at the molecular orbitals depicted in Figure 2 where the left- and rightmost orbitals represent the unmixed CH_2 and p orbitals, respectively. Strain is introduced by allowing θ to take on the values 120, 110, 90, and 60°; the other geometry parameters are given the STO-3G optimized values at $\theta = 120°$ (vide infra).

The simple MO picture given in Figure 2 really corresponds to a one-electron MO non-self-consistent field representation; that is, the foregoing type of argument does not incorporate electron repulsion effects.[10] Accordingly, calculations were first carried out at the extended Hückel theory (EHT) level.

EHT Calculations of Vinyl Cations. Standard EHT calculations[11] were carried out for the four vinyl cation structures described above. Figure 3 depicts the energies of the bonding MO (BMO) and antibonding MO (ABMO) and their energy difference, $\Delta\epsilon$. As expected, the BMO energy rises monotonically as θ is decreased. Surprisingly, however, the ABMO energy remains relatively constant but not monotonic until θ is less than 90°. To arrive at an explanation of this result we turn next to the energies of the separated CH_2 group and carbonium p orbital; that is, we consider orbital energies of these groups before the hyperconjugation interaction of Figure 1. There is no simple way of accomplishing such a separation in an SCF treatment because the individual SCF MO energies contain too much electron repulsion.[10] This problem does not occur in Hückel treatments in which such electron repulsion terms are not treated explicitly; hence, in the EHT approach we obtained this result by simply repeating each calculation with the two carbons separated by a long distance (50 Å). The
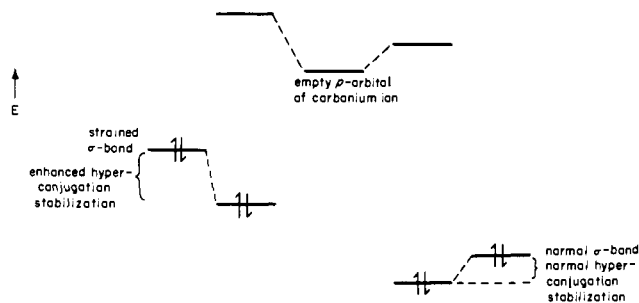
Figure 1. For equal overlaps a higher energy σ bond of appropriate symmetry is stabilized more by interaction with an empty p orbital than is a lower energy σ orbital.
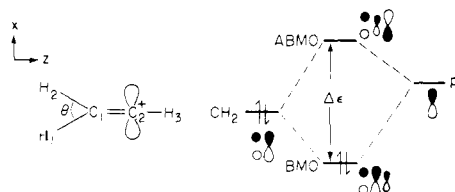

Figure 2. MO interaction diagram for vinyl cation.

Figure 3. EHT results as a function of HCH bond angle in vinyl cation. Shown are the BMO and ABMO energies and Δε ($\epsilon_{ABMO} - \epsilon_{BMO}$) compounds to the corresponding MO energies of the separated CH_2 group and p orbital. The Δε scale is on the right-hand margin.

Figure 4. Antibonding interactions in the ABMO.

Table I. Overlap Integrals in ABMO for Vinyl Cations (EHT)

θ, deg	S (H_{1s}–$C_{2px}^{(2)}$)	S (H_{1s}–H_{1s})
120	−0.0702	−0.1183
110	−0.0600	−0.1405
90	−0.0432	−0.2093
60	−0.0249	−0.4081

Table II. BMO and ABMO Energies of Vinyl Cations

θ, deg	ε(BMO)	ε(ABMO)	Δε
	EHT, eV		
120	−15.9467	−10.7180	5.2287
110	−15.7564	−10.7724	4.9840
90	−15.2471	−10.7511	4.4960
60	−14.1952	−9.9891	4.2061
	STO-3G, au		
120	−0.8933	−0.1723	0.7210
110	−0.8750	−0.1761	0.6989
90	−0.8330	−0.1774	0.6556
60	−0.7602	−0.1521	0.6081

BMO is now entirely the CH_2 group orbital and the ABMO is entirely a carbon 2p orbital. As shown in Figure 3 the p-orbital energy is independent of θ whereas the energy of the CH_2 group orbital increases as θ is decreased. The latter result is in part a manifestation of increasing antibonding overlap of the two CH_2 hydrogens as they approach each other with decreasing θ. In the ABMO a second antibonding overlap occurs between these hydrogens and the p orbital as symbolized in Figure 4. As θ decreases the distance between the hydrogens and the p orbital increases. These overlap effects are summarized in Table I. With a decrease in θ the antibonding interaction *a* in Figure 4 increases and that of *b* decreases *but to different degrees;* hence, the total MO energy is a nonmonotonic function of θ.

More important, however, is the bonding interaction between the CH_2 group and the p orbital. As anticipated in Figure 1, the results summarized in Figure 3 show that as θ is decreased from 120° and the energy of the CH_2 group orbital increases, the hyperconjugative interaction with the p orbital increases as reflected by the increase in the energy difference, $\epsilon(CH_2) - \epsilon(BMO)$. Thus, at least at the EHT level, the hyperconjugation effect of Figure 1 is confirmed. We next examine whether the effect is confirmed in ab initio SCF calculations and finally test the degree to which the effect contributes to the total energies and observable chemistry of several representative real systems.

STO-3G Calculations of Vinyl Cations. Calculations for the same vinyl cation calculations as above were also performed at the STO-3G level[12] using the Gaussian 70 program.[13] Meaningful calculations of SCF MO energies on the separated systems cannot simply be done here,[10] but an examination of the BMO and ABMO energies compared with EHT energies in Table II is instructive. These energies cannot be compared directly and we have emphasized this point by recording them in Table II in different units for EHT and STO-3G but their changes as a function of θ are meaningful and significant. The STO-3G BMO energies increase monotonically as θ is decreased as in the EHT calculations. More striking is the fact that the ABMOs also behave in the same manner in both sets of calculations. Thus, the introduction of electron repulsion as embodied in SCF–MO energy levels does not change the essential features of the differing overlap effects as θ is revised. This comparison gives additional credence to the EHT interpretation of the effect of strain on hyperconjugation. Expressed
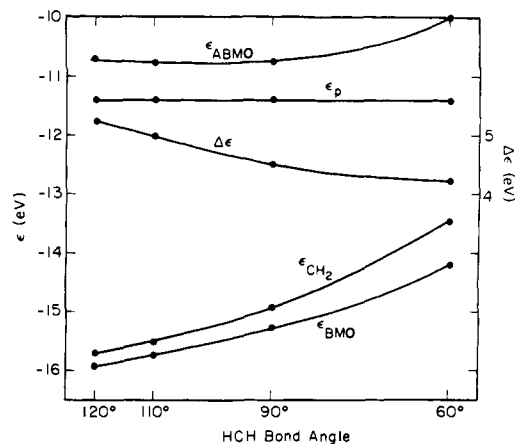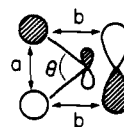
in this manner, there is no question but that the effect discussed in Figure 1 exists; however, there are other MOs in a molecule that are affected by strain and the key question is whether the indicated effect is large enough and sufficiently dominant to account for observed chemistry. For this purpose we next examine the calculated energy changes as a function of the strain angle for representative reactions that produce cations. All further calculations are at the STO-3G level. This entire approach complements our study of the effect of strain on the relative stabilities of carbanions.[14]

The first series of calculations involves the computed energy required to remove a hydride ion from a series of distorted ethylenes (I) to produce the corresponding vinyl cations (II).
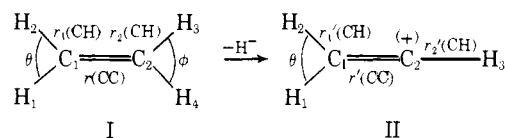
Table III. Hydride Affinities of Vinyl Cations

θ, deg	E_I, au	E_{II}, au	$\Delta E(I \rightarrow$ $H^- + II)$, kcal mol^{-1} [a]
130	$-77.067\ 28$	$-76.162\ 32$	468.4
120	$-77.073\ 32$	$-76.165\ 35$	470.3
110	$-77.072\ 79$	$-76.163\ 59$	471.1
90	$-77.048\ 67$	$-76.144\ 37$	468.0
60	$-76.932\ 23$	$-76.067\ 69$	443.0

[a] The energy of H^-, STO-3G, standard exponent, is $-0.158\ 56$ au.

Table VI. Calculated Energies for Optimized Ethylenes and Vinyl Cations

θ, deg	Total energies, au		$\Delta E(I \rightarrow H^- + II)$,[a] kcal mol^{-1}
	I	II	
130	$-77.067\ 30$	$-76.162\ 35$	468.4
120	$-77.073\ 32$	$-76.165\ 35$	470.3
110	$-77.072\ 85$	$-76.163\ 63$	471.1

[a] The energy of H^-, STO-3G, standard exponent, is $-0.158\ 56$ au.

Table VII. Percent s Contribution of C_1 to C_1C_2 Double Bond as a Function of θ

θ, deg	% s
130	21.51
120	23.61
110	25.51

The angle θ was fixed at the values 130, 120, 110, 90, and 60°. The parameters $r_1(CH)$, $r_2(CH)$, $r(CC)$, and ϕ were optimized for I (1.0811, 1.0821, 1.3096 Å, 115.6°, respectively) and $r_1'(CH)$, $r_2'(CH)$, and $r'(CC)$ were optimized for II (1.1062, 1.1057, 1.2815 Å, respectively) at the θ value of 120°; θ was the only variable in calculations at the remaining angles. The $C_1C_2H_3$ angle in II was taken to be 180° in all cases. The calculated energies of reaction are shown in Table III. For modest changes in θ the effects are rather small but we note that compression of the angle θ from 130 to 110° makes the formation of the carbonium ion somewhat *less* favorable, in apparent contrast to the effect pictured in Figure 1. Decreasing the angle below 110° does apparently cause dominance of the hyperconjugative effect and makes formation of the carbonium ion rather more favorable. To verify that the trend in ΔE where θ is 130, 120, and 110° is real and not due to the artificial constraint placed up on the system by not allowing full geometry optimization at each θ, the parameters noted above were optimized at each of the three angles; the results are summarized in Tables IV-VI. The same trend is found to hold exactly; that is, geometry optimization does not change the nonmonotonic nature of these hydride affinities. The optimized parameters and Mulliken populations at each of these three angles do provide an interesting insight, however, and their analysis shows the incursion of an opposing effect which dominates the hyperconjugative effect at small angle deviations from 120°.

As the angle θ is decreased in I, the p character of the C_1-H bond is increased and $r_1(CH)$ increases. Correspondingly, the s contribution of C_1 to the C_1-C_2 double bond increases resulting in shortening of $r(CC)$; this increase in s contribution is quantified in Table VII using the definition of % s character introduced previously[14] in terms of Mulliken overlap population, P_{ij}, between atomic orbital i on atom A and j on B:

Fraction s character of A in bond

$$A-B = \sum_{i=s}^{j=sp} P_{ij} \Big/ \sum_{i=s,p}^{j=s,p} P_{ij}$$

C_2 is, in effect, bonded to a more electronegative orbital and therefore requires greater energy to convert to a carbonium ion. The corresponding effect was shown previously to provide stabilization of the corresponding vinyl anion.[14] Other changes in I are consistent with these changes in s and p character of various localized orbitals. As the s contribution of C_1 to the C_1C_2 double bond increases, the C_2 contribution is expected to increase in p character;[15] more s character is thus available for the C_2-H bond resulting in an increase in θ and a decrease in $r_2(CH)$. These changes at C_2 are substantially smaller than those at C_1.

What all this means with reference to the hyperconjugation effect in Figure 1 is that this figure refers to only one molecular orbital out of many. For example, the five occupied valence MOs of vinyl cation are shown schematically in Figure 5. The stabilized σ orbital of Figure 1 corresponds to ψ_6 of Figure 5. The existence of hyperconjugation is shown by the electron projection plot[16] of ψ_6 (Figure 6). In this function, for each point in the xz (molecular) plane of II, the electron density, ρ, has been integrated along the y axis from $+\infty$ to $-\infty$ and the integrated function is plotted as a perspective plot. The total volume of the figure should correspond to two electrons, the total number of electrons in ψ_6. Numerical integration of

Table IV. Optimized Structure Parameters and Mulliken Populations for Distorted Ethylenes, I

Angles, deg		Optimized structures			Mulliken populations			
θ	ϕ	$r(CC)$, Å	$r_1(CH)$, Å	$r_2(CH)$, Å	C_1	C_2	H_1	H_3
130	115.30	1.3140	1.0798	1.0822	6.14	6.12	0.928	0.942
120	115.60	1.3096	1.0811	1.0821	6.13	6.125	0.934	0.938
110	115.85	1.3057	1.0832	1.0820	6.12	6.13	0.939	0.935

Table V. Optimized Structure Parameters and Mulliken Populations for Distorted Vinyl Cations, II

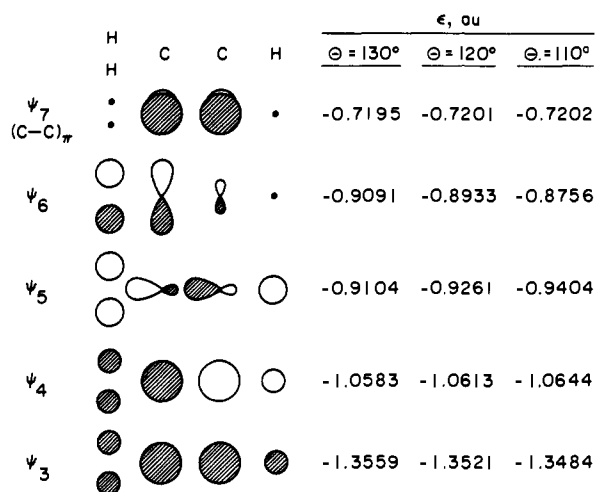| θ, deg	Optimized structures			Mulliken populations			
	$r(CC)$, Å	$r_1'(CH)$, Å	$r_2'(CH)$, Å	C_1	C_2	H_1	H_3
130	1.2862	1.1063	1.1066	6.05	5.72	0.753	0.724
120	1.2815	1.1062	1.1057	6.06	5.72	0.751	0.723
110	1.2763	1.1067	1.1059	6.07	5.72	0.746	0.722

Figure 5. The molecular orbitals of vinyl cation; energies reflect geometry-optimized vinyl cations. ψ_1 and ψ_2 are carbon core MOs 1σ and 2σ. Positive lobes are shaded.

Figure 6. Electron projection plot for ψ_6 in the molecular plane. The volume under any given surface gives directly the number of ψ_6 electrons in that region.

Figure 6 around each grid point actually gives 1.986e; the difference from 2e is the error associated with the numerical integration. Hyperconjugation provides the hump of electron density at C_2 which is clearly visible in this figure. If it were possible to define the boundary between carbons, one could determine spatial electron populations for each atom. Atomic charges are not physical observables and any such definition involves some degree of arbitrariness.[17] One approach is to mark the boundaries at the covalent radii of the carbon atoms, 0.61 Å for C_{sp} and 0.67 Å for C_{sp^2}.[18] With this definition, numerical integration gives 0.143e at C_2 and 1.843e for the CH_2 group; that is, hyperconjugation results in a charge transfer of 0.143e from CH_2 to the "empty" 2p orbital at C_2. Note that H_3 does not contribute to ψ_6 in a minimum basis set because it lies on a nodal plane.

The significance of the foregoing treatment is that it establishes the validity of hyperconjugative charge delocalization as a real phenomenon not limited by the known inadequacies of Mulliken populations.[17] Nevertheless, although hyperconjugation clearly exists in this model and the effect illustrated in Figure 1 must result in increased hyperconjugative stabilization of the carbonium ion, changes are also produced in other molecular orbitals that can be regarded as polarization or electronegativity changes and result in compensating energy increases. The net effect is a balance between these opposing energy effects that, in the case of small angle changes from 120°, results in a net increase, albeit rather small, in the energy required to remove a hydride ion from the methylene group of an ethylene molecule in which the adjacent methylene group is constrained to a reduced bond angle. For larger deviations, the energy changes in ψ_6 dominate all other changes, the hyperconjugative stabilization becomes of overriding importance, and loss of a hydride ion becomes more facile. Indeed, the initial increase in energy is sufficiently small that the actual number might well be basis set dependent, but the trend is probably accurate and the inadequacy of an interpretation based solely on the hyperconjugation effect of Figure 1 is clearly established.

Isopropyl Cation. In the next reaction, we examine the protonation of propylene (III) to 2-propyl cation (IV) in which
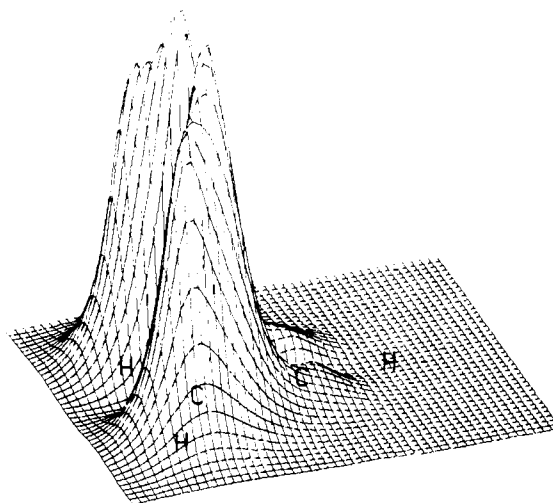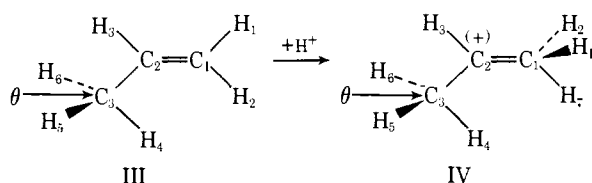

III   IV

Table VIII. Structural Parameters of Constrained Propenes (III)

θ, deg	$r(C_1-C_2)$, Å	$r(C_2-C_3)$, Å	$r(C_3-H_5)$, Å	$r(C_3-H_4)$, Å
113.5	1.3084	1.5249	1.0870	1.0857
105	1.3084	1.5205	1.0885	1.0844
90	1.3085	1.5129	1.0935	1.0821
60	1.3092	1.4955	1.1220	1.0754

Table IX. Structural Parameters of Constrained 2-Propyl Cations (IV)

θ, deg	$r(C_1-C_2)$, Å	$r(C_2-C_3)$, Å	$r(C_3-H_5)$, Å	$r(C_3-H_4)$, Å
113.5	1.4989	1.5027	1.0958	1.0884
105	1.4989	1.4953	1.0967	1.0870
90	1.4991	1.4780	1.1015	1.0845
60	1.5035	1.4182	1.1412	1.0796

Table X. Calculated Energies for Propenes and 2-Propyl Cations

θ, deg	Total energies, au III	Total energies, au IV	Proton affinities ΔE, kcal mol^{-1}
113.5	−115.658 91	−116.025 83	230.2
105	−115.659 92	−116.027 14	230.4
90	−115.647 86	−116.018 27	232.4
60	−115.557 18	−115.955 40	249.8

one methylene group in both reactant and product is constrained to a distorted angle, θ. This reaction allows us to model the effect of strain on an adjacent sp^2 cationic center. The $H_5C_3H_6$ angle was constrained in both III and IV to values of 113.5, 105, 90, and 60° and selected structural parameters were optimized at the STO-3G level. It was impractical to optimize all structural parameters. Only the following bond distances were optimized for both III and IV: $C_3-H_5 = C_3-H_6$, C_3-H_4, C_2-C_3, C_1-C_2. Other bonds and angles were taken as the optimal values of Pople et al. for propene[19] and 2-propyl cation.[20] The results are summarized in Tables VIII-X.

A small change in the methylene bond angle has but a small effect on the proton affinity of constrained propene, but a larger bond angle decrease makes the protonation reaction substantially more favorable. For small bond angle changes the hyperconjugative and electronegativity effects approxi-

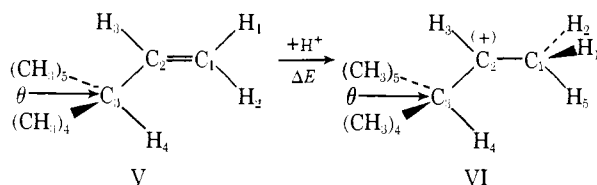**Table XI.** Calculated Energies for the 3-Methyl-2-butyl System

θ, deg	Total energies, au		Proton affinities ΔE, kcal mol^{-1}
	V	VI	
113.5	−192.818 78	−193.195 12	236.2
105	−192.817 38	−193.193 31	235.9
90	−192.786 42	−193.165 14	237.6
60	−192.227 49	−192.646 20	262.8

Table XII. Orbital Population of "Empty" 2p Orbital on 3-Methyl-2-butyl Cation

θ, deg	Electron population, e
113.5	0.201
105	0.213
90	0.248
60	0.518

Table XIII. Calculated Energies for the Para-Protonated Tolyl System

θ, deg	Total energies, au		Proton affinities ΔE, kcal mol^{-1}
	VII	VIII	
113.5	−266.472 76	−266.848 04	235.5
105	−266.473 63	−266.848 57	235.3
90	−266.461 24	−266.836 68	235.6
60	−266.367 96	−266.752 09	241.1

Table XIV. Orbital Population of 2p Orbitals on Tolyl Cation

θ, deg	C_1, e	C_3, e	C_5, e
113.5	0.692	0.614	0.698
105	0.693	0.616	0.698
90	0.694	0.619	0.700
60	0.705	0.624	0.709

mately cancel each other but for seriously reduced bond angles, the hyperconjugation effect clearly dominates.

3-Methyl-2-butyl Cation. The above examples have an important limitation as models of real strained systems. In such systems, the hyperconjugation involved is typically that of a small carbocyclic ring in which C–C rather than C–H hyperconjugation is involved. Calculations were thus undertaken on the 3-methyl-2-butyl cation. In a manner analogous to the 2-propyl case, the $C_5C_3C_6$ angle was constrained in both V and VI to the angles 113.5, 105, 90, and 60°. Aside from the $(CH_3)_5$–C_3–$(CH_3)_6$ parameters, all values at each θ were taken from the optimized propene–propyl system; the bond distances and bond angle in the $(CH_3)_5$–C_3–$(CH_3)_6$ moiety were taken as the standard values.[21] The results are shown in Table XI.

As may be seen, a substantial decrease in θ results in the protonation becoming more favorable, pointing to a dominance of the hyperconjugative effect—as was the case when we were seeing C–H hyperconjugation. For smaller changes in θ, the situation is not so clear cut. The monotonic increase in the calculated proton affinity of the strained olefin in going from 113.5 to 90° is probably real and, correspondingly, the hyperconjugative mechanism progressively dominates with increasing angle strain; however, the +0.3 kcal mol^{-1} change in going from 113.5 to 105° is so small as to have dubious reliability. For such small angle changes the hyperconjugative and electronegativity mechanisms make approximately equal and opposite contributions. It should be noted that the population of the "empty" 2p orbital on C_2 steadily increases as a function of decreasing θ with the change being +0.047e in going from 113.5 to 90° and 0.270e in going from 90 to 60° (see Table XII).

It has been shown in a variety of cases that C–C hyperconjugation is more important than C–H hyperconjugation in stabilizing a cationic center;[22] however, the essential conclusion of the foregoing results is that angle changes produce comparable energy changes in both series.
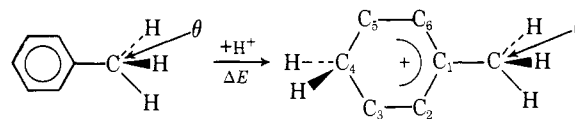
Para-Protonated Toluene. Having established a parallel between C–C and C–H hyperconjugation, a final set of STO-3G calculations was done on the para-protonated tolyl

cation. Standard geometries were used throughout;[21,23] protonation of toluene has previously been shown to favor the para position.[24] This case has special significance because the calculated proton affinities of para-substituted benzenes have been shown to correlate well with corresponding σ^+ values.[25] Moreover, this reaction is a model of the benzoylation reaction of Jensen and Smart,[2] who found that 1-phenylnorbornane undergoes electrophilic benzoylation faster than either *exo*- or *endo*-2-phenylnorbornane; their explanation was that in the 1-phenylnorbornane, the strained C–C bonds can enter more readily into hyperconjugative interaction with the positively charged ring and thus stabilize the transition state. The present calculations provide a direct determination of the effect of angle strain on the energy of the model reaction. The results are summarized in Table XIII. Again, a substantial reduction in θ results in more favorable protonation. The situation is not so clear for smaller changes in θ around 105° and may again be evidence of the competing hyperconjugative and electronegativity mechanisms, especially in light of the monotonic increase in 2p orbital population found in the 3-methyl-2-butyl case and a similar trend found here for the 2p orbitals on carbons 1, 3, and 5 as seen in Table XIV. A relationship between increasing strain and a more effective stabilization of a positive charge is thus determined theoretically.

Conclusion

An analysis has been presented of the effect of bond angle change within a hyperconjugating group in a carbonium ion on the energies of the corresponding bonding and antibonding MOs; a decrease in bond angle results in increasing hyperconjugation and a decrease in the energy of the bonding MO. However, other changes occur in the remaining molecular orbitals such that the overall energy difference of related model reactions show no simple relationship with hyperconjugation alone. This example points up the limitations of MO interpretations based solely on HOMO and LUMO interactions.

References and Notes

(1) This research was supported in part by USPHS–NIH Grant GM-12855 and NSF Grant CHE 76-10997. Additional computer time was donated by the Computer Center, University of California, Berkeley.
(2) F. R. Jensen and B. E. Smart, *J. Am. Chem. Soc.*, **91**, 5686 (1969).
(3) N. A. Clinton, R. S. Brown, and T. G. Traylor, *J. Am. Chem. Soc.*, **92**, 5228 (1970); T. G. Traylor, W. Hanstein, H. J. Berwin, N. A. Clinton, and R. S.

Brown, *ibid.*, **93**, 5715 (1971); D. F. Eaton and T. G. Traylor, *ibid.*, **96**, 1226 (1974); and prior references cited in those papers.

(4) L. Radom, J. A. Pople, and P. v. R. Schleyer, *J. Am. Chem. Soc.*, **94**, 5935 (1972).

(5) G. A. Olah and R. J. Spear, *J. Am. Chem. Soc.*, **97**, 1539 (1975); G. A. Olah, C. L. Jeuell, D. P. Kelly, and R. D. Porter, *ibid.*, **94**, 146 (1972).

(6) J. J. Solomon and F. H. Field, *J. Am. Chem. Soc.*, **98**, 1567 (1976).

(7) G. A. Olah, A. M. White, J. R. DeMember, A. Commeyras, and C. Y. Lui, *J. Am. Chem. Soc.*, **92**, 4627 (1970); G. A. Olah, G. D. Mateescu, and J. L. Riemenschneider, *ibid.*, **94**, 2529 (1972).

(8) H. C. Brown, *Acc. Chem. Res.*, **6**, 377 (1973).

(9) For other experimental and theoretical work on the vinyl cation see J. Weber and A. D. McLean, *J. Am. Chem. Soc.*, **98**, 875 (1976); P. C. Hariharan, W. A. Lathan, and J. A. Pople, *Chem. Phys. Lett.*, **14**, 385 (1972); A. C. Hopkinson, K. Yates, and I. G. Csizmadia, *J. Chem. Phys.*, **55**, 3835 (1971); Z. Rappoport, I. Schnabel, and P. Greenzaid, *J. Am. Chem. Soc.*, **98**, 7726 (1976), and references cited therein; P. J. Stang, *Prog. Phys. Org. Chem.*, **10**, 205 (1973).

(10) This limitation has long been known. For a recent review and discussion applied to Walsh's rules, see R. J. Buenken and S. D. Peyerimhoff, *Chem. Rev.*, **74**, 127 (1974). E. R. Davidson [*J. Chem. Phys.*, **57**, 1999 (1972)] has defined an alternative set of canonical orbitals within the Roothaan–Hartree–Fock formalism and has shown [L. Z. Stenkamp and E. R. Davidson, *Theor. Chim. Acta*, **30**, 283 (1973)] how such SCF orbital energies can be applied to molecular changes of the Walsh type.

(11) R. Hoffmann, *J. Chem. Phys.*, **39**, 1197 (1963); R. Hoffmann, R. Piccioni, and R. Fahey, Program No. 48, QCPE, Indiana University, Bloomington, Ind.

(12) W. J. Hehre, R. F. Stewart, and J. A. Pople, *J. Chem. Phys.*, **51**, 2657 (1969).

(13) W. J. Hehre, W. A. Lathan, R. Ditchfield, M. D. Newton, and J. A. Pople, Program No. 236, QCPE, Indiana University, Bloomington, Ind.

(14) A. Streitwieser, Jr., P. H. Owens, R. A. Wolf, and J. E. Williams, *J. Am. Chem. Soc.*, **96**, 5448 (1974); P. H. Owens and A. Streitwieser, Jr., *Tetrahedron*, **27**, 4471 (1971).

(15) H. A. Bent, *Chem. Rev.*, **61**, 275 (1961).

(16) A. Streitwieser, Jr., J. M. McKelvey, and A. G. Toczko, in preparation; for a specific example, see A. Streitwieser, Jr., J. E. Williams, Jr., S. Alexandratos, and J. M. McKelvey, *J. Am. Chem. Soc.*, **98**, 4778 (1976).

(17) J. E. Williams and A. Streitwieser, Jr., *Chem. Phys. Lett.*, **25**, 507 (1974); P. Politzer and R. R. Harris, *J. Am. Chem. Soc.*, **92**, 6451 (1970); R. S. Mulliken, *J. Chem. Phys.*, **36**, 3428 (1962).

(18) O. Bastiansen and M. Traetteberg, *Tetrahedron*, **17**, 147 (1962).

(19) L. Radom, W. A. Lathan, W. J. Hehre, and J. A. Pople, *J. Am. Chem. Soc.*, **93**, 5339 (1971).

(20) L. Radom, J. A. Pople, V. Buss, and P. v. R. Schleyer, *J. Am. Chem. Soc.*, **94**, 311 (1972); P. C. Hariharan, L. Radom, J. A. Pople, and P. v. R. Schleyer, *ibid.*, **96**, 599 (1974).

(21) J. A. Pople and M. S. Gordon, *J. Am. Chem. Soc.*, **89**, 4253 (1967).

(22) L. Radom, *Aust. J. Chem.*, **27**, 231 (1974).

(23) W. J. Hehre, R. T. McIver, J. A. Pople, and P. v. R. Schleyer, *J. Am. Chem. Soc.*, **96**, 7162 (1974).

(24) J. L. Devlin III, J. F. Wolf, R. W. Taft, and W. J. Hehre, *J. Am. Chem. Soc.*, **98**, 1990 (1976).

(25) J. M. McKelvey, S. Alexandratos, A. Streitwieser, Jr., J. L. M. Abboud, and W. J. Hehre, *J. Am. Chem. Soc.*, **98**, 244 (1976).

A Theoretical Relation for the Position of the Energy Barrier between Initial and Final States of Chemical Reactions

Arnold R. Miller[1]

Contribution from the Department of Chemistry, State University of New York at Stony Brook, Stony Brook, New York 11794. Received December 29, 1975; revised and expanded July 25, 1977.

Abstract: A function ψ is derived that approximates the potential-energy barrier position x^*_0 of elementary reactions in terms of the barrier height U^* and reaction potential energy U_f. The functional expression is $x^*_0 = 1/[2 - (U_f/U^*)]$, where x^*_0 is the value of the defined reaction coordinate x, $0 \leqslant x \leqslant 1$, that corresponds to the activated state; endpoints $x = 0$ and $x = 1$ correspond to the initial and final states, respectively. For three-body atom transfer reactions, x^*_0 is equal to the activated-complex bond order of the bond being formed. The central idea of the derivation is a proposition that the most realistic global interpolating function of a family, all of whose members equally well interpolate the potential coordinate function of the vector equation describing the minimum-energy reaction path, is the unique member having the least arc length for its potential curve or graph. This criterion may be considered an abstract, generalized basis for the well-known Hammond postulate. Relation ψ is tested principally by (a) graphical comparison with analogous functions generated numerically from the bond-energy/bond-order (BEBO) and London–Eyring–Polanyi–Sato (LEPS) potential functions, and (b) comparison of the saddle-point coordinates computed by the function with those computed by other methods, including ab initio methods. Agreement is good, and, as a generalization, the relation's predicted barrier position is very similar to that of the BEBO function.

Introduction

The position of the energy barrier over configuration space is one of the dynamically most important properties of a potential-energy surface.[2] Interest in the barrier position (i.e., the position of the barrier maximum) arises principally because of its profound effect on reaction rate. For example, the barrier position determines the *kind* of energy which will promote the reaction. Elementary three-body reactions having early barriers, or barriers in the entrance channel of the surface, are much more effectively promoted by reactant translational energy than vibrational energy, and, in striking cases, reactant vibrational energy even in excess of twice the barrier height gives no reactive trajectories whatever.[3] This effect of energy selectivity by the barrier position is of importance not only to the rates of elementary reactions but to the rates of (disequilibrium) reaction networks in which the reactant energy distribution for one elementary step is provided by the product energy distribution of the preceding step. That is, the rate of

the network will depend in part on the relative barrier positions of the elementary steps. As another example, the rate acceleration of solvation depends strongly on the barrier position since the latter determines the structure and electrostatic charge of the activated state. For instance, it has been predicted for an ionogenic reaction (the Menschutkin reaction) that the rate enhancement accompanying a given change in solvent (all other variables held constant) will vary from a factor of 10 to a factor of 10^{10} depending on the barrier position.[4]

There is presently no unambiguous experimental method of determining the barrier position. Two experimental reaction parameters commonly related to the barrier position are the Brønsted slope[5] and the kinetic isotope effect.[6] However, the validity of these methods is generally uncertain because of the uncertainty of the multiple assumptions upon which they rest. The method nearest to being a bona fide experimental method involves the construction of an adjustable, semiempirical potential-energy surface that properly reproduces a given reaction's experimentally observed dynamics, for example, the